

## Paleomagnetic results from the Cambrian-Ordovician boundary section at Black Mountain, Georgina Basin, western Queensland, Australia

Robert L. Ripperdan & Joseph L. Kirschvink  
*California Institute of Technology, Pasadena, Calif., USA*

**ABSTRACT:** Zones of alternating magnetic polarity have been identified throughout the Cambrian-Ordovician sequence at Black Mountain, and can be presumed to record geomagnetic field reversals during or immediately after deposition. A strong correlation can be made to polarity zones recognized at Dayangcha, northeastern China, a candidate site for establishment of the Cambrian-Ordovician boundary Global Stratotype Section and Point. Polarity zones associated with the *Hispidodontus discretus* and *Hirsutodontus simplex* Assemblage-Zones at Black Mountain are absent at Dayangcha, suggesting hiatuses at these levels in the Dayangcha sequence. Secondary components preserved in the Black Mountain section may provide temporal constraints on Middle Paleozoic diagenetic events in the Burke River Structural Belt.

### 1 INTRODUCTION

The designation of a Global Stratotype Section and Point (GSSP) for the Cambrian-Ordovician boundary has been the subject of an international effort for nearly twenty years. In 1986, the Cambrian-Ordovician Boundary Working Group resolved to establish a conodont-based GSSP in either northeastern China or western Newfoundland, Canada. Final agreement has not been forthcoming, however, because of difficulties in establishing reliable first appearance data (FAD) for both the *Cordylodus proavus* and *Cordylodus lindstromi* Assemblage-Zones, the most favored boundary levels, and the possibility of significant hiatuses within the boundary interval in both of the candidate sections. The work reported here is part of a wider effort to establish non-biological correlations within the boundary interval (Ripperdan 1990; Ripperdan et al., in review), in hopes of resolving these problems and establishing firm temporal constraints for global correlation of a Cambrian-Ordovician GSSP.

A primary reason for attempting to construct a geomagnetic polarity time scale through the

boundary interval is the observation that the geomagnetic field has the same polarity simultaneously over the entire Earth's surface, except during geologically very brief periods (<5,000 years) of polarity reversal (Harrison & Somayajulu 1966; Opdyke et al. 1973; many others). When used within a suitable stratigraphic framework, magnetic polarity reversals are therefore potential "absolute time" markers capable of accurately correlating sections without the difficulties imposed by facies-dependent or endemic faunas. Their use is hampered in pre-Mesozoic rocks, however, by the need to establish a reference magnetic polarity time scale, since the marine magnetic lineation record extends back only to the Middle Jurassic (Harland et al. 1989). Therefore, the magnetic polarity time scale must be assembled from a number of well-documented, overlapping sections. This is best achieved using biostratigraphically-constrained sections that are thick, well-exposed, and free of apparent unconformity or hiatus; and that have not been subjected to extreme heating or deep burial, effects that can destroy the primary magnetization of sedimentary rocks. These criteria are

generally satisfied by the section at Black Mountain.

In this study we suggest that a component recording the depositional or immediately post-depositional geomagnetic field is preserved within the sequence at Black Mountain, as are components related to later periods of diagenesis and exposure. From this, we have determined a preliminary magnetic polarity time-scale for the Cambrian-Ordovician boundary interval that is correlatable to similar-aged localities, including one of the candidate sections for establishment of the Cambrian-Ordovician GSSP.

## 2 GEOLOGIC SETTING

Black Mountain (Unbunmaroo) is the northernmost of three elongate, faulted domes that are the major features of the southern part of the Burke River Structural Belt (Fig. 1). Movement along the Black Mountain Fault immediately to the east has exposed a thick sequence of Upper Cambrian and Lower Ordovician sediments. Two formations are present: the upper third of the Chatsworth Limestone, which is comprised of a series of upwards-shallowing carbonate sequences; and the Ninmaroo Formation, a thick, predominantly carbonate unit extending over much of the southeastern Georgina Basin (Druce et al. 1982). The type section for the Ninmaroo Formation is at Black Mountain. Units near the top of the Chatsworth Limestone reflect restricted marine circulation (Druce et al. 1982), and there is strong evidence for epeiric marine and saline conditions throughout the overlying Ninmaroo Formation (Radke 1980, 1981, 1982). Carbon isotope data suggests the lower two-thirds of the Chatsworth Limestone at Black Mountain were deposited in a more stable marine setting (Ripperdan et al., in review).

Black Mountain has played an important role in Australian chronostratigraphy since 1971, when Jones, Shergold, and Druce integrated conodont and preliminary trilobite biostratigraphies and recognized three stages across the boundary interval (Jones et al. 1971). The section was further documented by subsequent studies (Shergold 1975, 1980, 1982; Pojeta et al. 1977; Druce 1978; Runnegar et al. 1979; Druce et al. 1982), including the development of a new conodont zonation based on previously-unrecognized taxa below the *Cordylodus proavus* Assemblage-Zone and improved recoveries of taxa throughout the section (Nicoll & Shergold 1991; Shergold & Nicoll, this volume). These works facilitated correlations with the well-established conodont zonation from North American cratonic sections (see Miller 1984) and the trilobite-bearing sequences of the Sino-Korean Platform (see Kobayashi 1969), and clarified relationships to the generally accepted concept of the Cambrian-Ordovician boundary within the Acado-Baltic realm (Nicoll & Shergold 1991; see also Henningsmoen 1973). It has recently been suggested that Black Mountain has

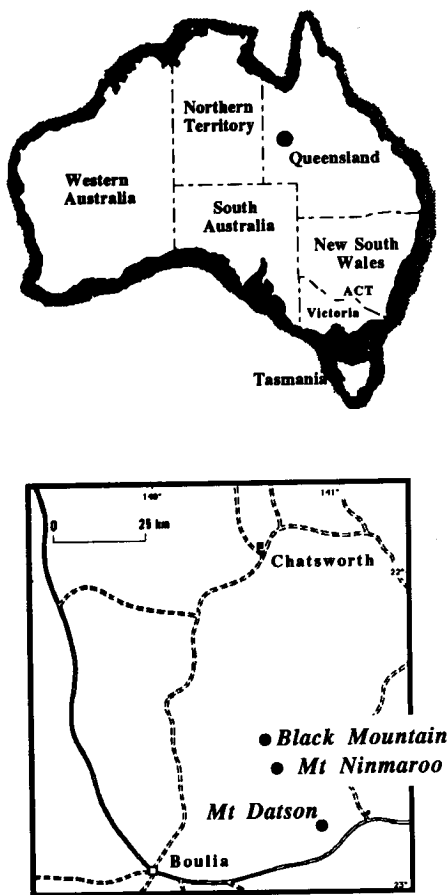


Fig. 1. Generalized locality map for Black Mountain (adapted from Nicoll & Shergold 1991).

the most complete conodont sequence yet found spanning the boundary interval (Shergold & Nicoll, this volume), based on splits of samples used in the work reported here.

One of the appealing aspects of the section is the thickness of the sequence preserving the boundary interval. Over 200 meters of section are found between the bases of the *Cordylodus proavus* and *Cordylodus lindstromi* Assemblage-Zones (Shergold & Nicoll, this volume); the same interval is contained within less than 15 meters at the GSSP-candidate section at Dayangcha, China (Repetski, Ethington & Taylor, COBWG Circular 27, Appendix 3). Also, examination of conodont color gives a conodont alteration index (CAI) value of 1.0-1.5 (R.S. Nicoll, pers. comm.), indicating maximum temperatures of around 100° (Epstein et al. 1977). It is therefore considered extremely unlikely that thermal remagnetization components contribute significantly to the preserved magnetization. Because of these features, the section provides an exceptional opportunity for high-resolution geomagnetic polarity stratigraphy precisely calibrated against a detailed biostratigraphy.

### 3 RESULTS

#### 3.1 Methods and techniques

One hundred seventeen oriented block samples (BMA set) were collected at approximately equal intervals from the section in August, 1989. An additional 52 samples (BMA set) were collected from previously unsampled units in the upper half of the Ninmaroo Formation by a Bureau of Mineral Resources field party in 1990. The blocks were cored, with the remainders of the blocks dissolved for conodont investigations by R.S. Nicoll at the Bureau of Mineral Resources, Canberra, Australia. The cores were subsequently cut to 2.5cm x 2.5cm cylinders and rinsed in 1N HCl. Unrinsed endchips were used for carbon isotope studies (Ripperdan et al., in review).

Paleomagnetic measurements were carried out in a shielded room using an ScT cryogenic magnetometer equipped with 2G SQUID electronics and interfaced to a dedicated microcomputer. Thermal demagnetizations were performed on all samples using 25° C. increments (50° C. for samples at the top of the

section) up to 600° C. using a custom-built oven. A few samples were subjected to alternating-field demagnetization using a 2G AF demagnetizer. Field increments of 2.5mT were used, with a maximum intensity of 50 mT.

Isothermal remanent magnetization (IRM) acquisition-AF demagnetization studies were carried out using a custom-built IRM pulse demagnetizer capable of field intensities in excess of 0.8 Tesla. Goethite and hematite were distinguished from magnetite by unsaturation of magnetization at IRM fields in excess of 0.5 T, and from each other by absence/presence of a high-coercivity component after heating at 150°.

Characteristic directions were determined using principal component techniques outlined in Kirschvink (1980).

#### 3.2 Data

Intensities of natural remanent magnetization (NRM) were typically within the range of  $10^{-8}$  to  $10^{-10}$  Am<sup>2</sup>. Most samples had NRM vectors similar to the present-day geomagnetic field direction in western Queensland (Fig. 2). Clustering around the present-day direction was significantly improved using the vector of initial magnetization loss (IML). The similarity of the IML component directions to the present-day geomagnetic field direction suggests that a strong component of NRM is

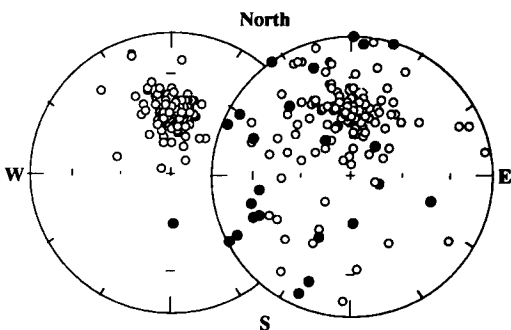


Fig. 2. NRM directions (right) and initial magnetization loss vectors. Open circles represent negative (up) inclinations. Not corrected for tilt of bedding.

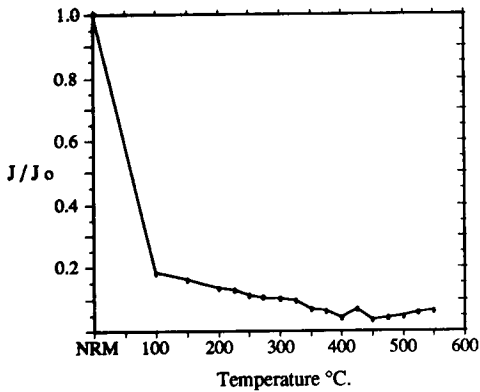


Fig. 3.  $J/J_0$  plot for sample BMA 4. The rapid dropoff in intensity with initial heating is typical of samples from this section.

preserved in a low-thermal stability authigenic mineral of modern origin or as a viscous remanent magnetization (VRM).

Samples with stronger NRM's usually experienced a rapid loss of intensity at the onset of thermal demagnetization (Fig. 3), probably due to the breakdown of goethite or the unblocking of very fine grains of hematite. Progressive demagnetization yielded shifts away from the modern field direction towards shallower inclinations in most samples. Typically, a characteristic component was isolated by low

levels of thermal demagnetization and remained stable (although often weak) up to 350-400° C. (Fig. 4a). IRM-AF acquisition studies indicated magnetite was the likely carrier of this component. Subsequent thermal demagnetization often led to the development of a dominating chemical remanent magnetization (CRM) carried by a high-coercivity mineral, probably hematite.

A number of samples exhibited simple one-component demagnetization trajectories nearly due south or northwest and equatorial that remained stable to 500° C. or above (Fig. 4b). Hematite appears to be the principle carrier of remanence in these samples.

The directions of magnetization components fall into three broad groups: those parallel to the modern field (the IML group); those with shallow inclination and west (east)-trending directions (CO1°); and those with shallow inclination, south or northwest-trending directions (OVP<sup>1</sup> and OVP<sup>2</sup>) (Table 1). The CO1° and OVP components were distinguished on the basis of direction and stability of the isolated direction during demagnetization. OVP<sup>1</sup>-group directions are distinct from CO1°-group directions, whereas some overlap exists between the OVP<sup>2</sup> and CO1° distributions (Fig. 5).

Magnetic mineralogy was the primary criterion for distinguishing between CO1° and OVP-group directions on the peripheries of their respective distributions. Samples with

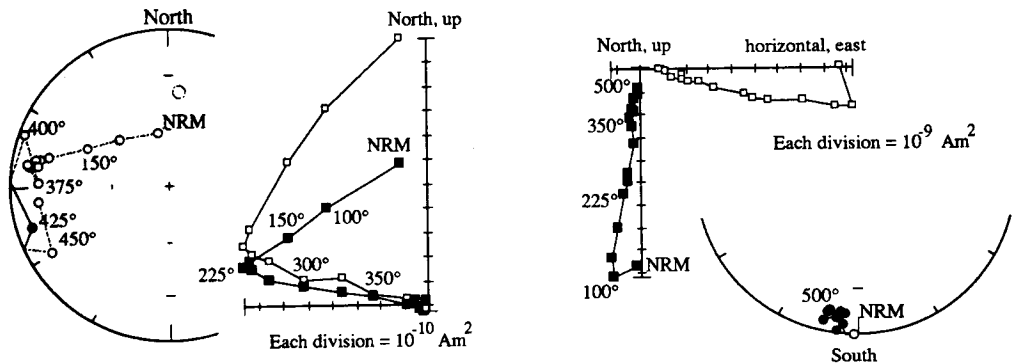


Fig. 4. Equal area and orthogonal projections of demagnetization trajectories typical of typical CO1° (a) and OVP1 samples. Equal area symbols as in Fig. 2. Filled squares represent declination, open squares represent inclination in orthogonal projection. Note that (b) is a hyperbolic projection to facilitate viewing. Corrected for tilt of bedding.

Table 1. Summary of section parameters from Black Mountain (22.6° S., 140.3° E.)

Group	Number of samples	Mean direction		Fisher statistics			Bingham statistics			
		Dec.	Inc.	$\kappa$	$\alpha_{95}$	$\kappa^1$	$\kappa^2$	$\alpha_{min}$	$\alpha_{max}$	ov. az.
CO1°	64 {16}	274.5	4.3	6.7	7.4	-5.7	-3.8	6.5	8.3	166.2
		(271.6)	24.2	5.8	8.1	-5.1	-3.3	7.1	9.3	169.7)
OVP <sup>1</sup> (south)	17	199.9	-7.5	10.7	11.4	-11.5	-5.1	8.0	12.5	208.9
		(204.7)	-14.8	8.8	12.7	-9.9	-4.3	8.8	14.1	172.5)
OVP <sup>2</sup> (northwest)	8	333.5	-17.7	10.7	15.5	-25.1	-5.2	7.2	16.6	171.7
		(330.5)	5.8	9.9	16.2	-34.3	-4.9	6.1	17.3	178.5)
IML	121	(359.9)	-52.8	35.2	2.2	-26.0	-14.4	1.8	2.5	152.8)

The number of samples with normal polarity is given in brackets. Dec. and Inc. refer to declination and inclination; ov. az. is the azimuth of the long axis of the oval of 95% confidence around the mean direction. Site parameters in parentheses are without structural correction.

lower unblocking temperatures were assigned to the CO1° group; samples stable at higher temperatures (~500° and above) were assigned to the appropriate OVP group. This distinction was principally based on the observation that high unblocking temperature associated with a high coercivity mineral was a common feature of samples with south-directed demagnetization paths, but was extremely rare in samples trending due west or east.

#### 4 Interpretation

The CO1° component directions are considered to reflect the geomagnetic field at the time of deposition based on a number of lines of experimental evidence. The CO1° directions satisfy the reversal test of McFadden and McElhinny (1990) at the 95% level (Table 2), indicating the hypothesis that the two polarities are drawn from a common population cannot

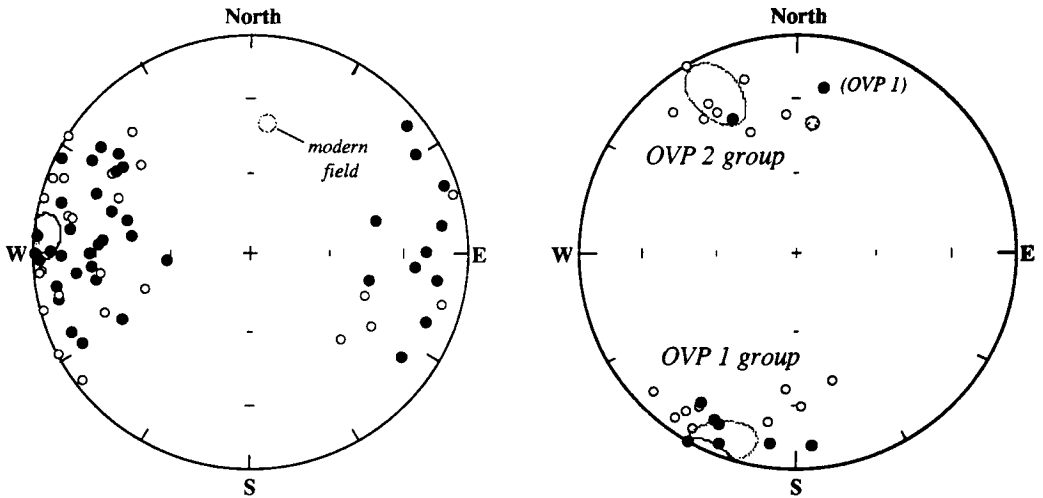


Fig. 5. Equal area projection of CO1° (left) and OVP component directions. Symbols as in Fig. 2. Directions have been corrected for dip of bedding.

**Table 2.** Reversal test based on the CO1° component.

polarity	N <sub>i</sub>	R <sub>i</sub>	Dec.	Inc.	a <sub>95</sub>
normal	16	13.3	92.6	6.0	17.0
reversed	48	42.4	275.1	8.2	8.2

$\gamma_0 = 165.6^\circ$ ;  $\gamma_c = 163.8^\circ$ ;  $\gamma_0 > \gamma_c = +$  reversal test

Abbreviations as in Table 1. Also, R<sub>i</sub>=length of vector sum of N<sub>i</sub> unit vectors for polarity i;  $\gamma_0$  is the observed angle between the two mean directions;  $\gamma_c$  is the critical angle greater than which the hypothesis of a common mean direction may be rejected at the 95% level (after McFadden and McElhinny 1990).

be rejected (although the utility of this comparison is partially restricted by the small number of directions having normal polarity). The identification of low-unblocking temperature magnetite as the principal remanence carrier of CO1° directions suggests a more primary origin for this component than for the OVP components; low-unblocking temperature magnetite is a common carrier of remanence in modern marine carbonates, as opposed to hematite.

A strong argument in favor of the CO1° component being primary is the stratigraphic grouping of normal polarity samples. Most of the normal polarity samples occur in discrete groupings at the 250-300 meter level within the Chatsworth Limestone, and at various levels within the Ninmaroo Formation (Fig. 6). The polarity is independent of significant shifts in carbon or oxygen isotopic signatures (Ripperdan et al., in review), suggesting that stratigraphically-bound diagenetic processes are not responsible for the observed polarity pattern. In contrast, half of the samples with OVP<sup>1</sup> or OVP<sup>2</sup> directions are found within 50 meters of the Chatsworth Limestone-Ninmaroo Formation contact, a zone interpreted to be a likely conduit for post-depositional diagenetic fluids.

Another argument favoring an early acquisition age of the CO1° component can be made through comparisons with the apparent polar wander (APW) track for Australia (Morel & Irving 1978; Li et al. 1990). The Cambrian-Ordovician portion of the track is a hairpin reflecting a period when Australia underwent

rapid counterclockwise rotation. Younger portions of the path (during the Paleozoic) do not overlap this hairpin, so presumed Cambrian-Ordovician pole positions lying within this APW hairpin should be strong evidence for a primary origin of the component. A pole position derived from the CO1° group (Table 3) lies directly on the Cambrian-Ordovician hairpin in the Australian APW path of Morel & Irving (1978), whereas pole positions derived from the OVP groups lie upon later portions of the track (Fig. 7).

## 5 DISCUSSION

### 5.1 Magnetostratigraphy

Reversed polarity is characteristic of the lower 850 meters of the Black Mountain section, with relatively short normal polarity magnetozones at various levels in the Ninmaroo Formation and at 250-300 meters in the Chatsworth Limestone (Fig. 6). Normal polarity is characteristic of strata above 850 meters. The uppermost sample of the section, at the base of the *Cordylodus angulatus* Assemblage-Zone, has reversed polarity.

One of the more problematic aspects of the geomagnetic polarity pattern recovered from Black Mountain is the presence of single sample normal polarity zones. The lowest one in the Ninmaroo Formation (BMA 86) is one sample above the base of the *Cordylodus proavus* Assemblage-Zone, a level that has been interpreted as a hiatus in other sections (Miller 1984). Of obvious interest is the possibility

**Table 3.** Pole positions from Black Mountain.

Component	Lat.	Long.	$\delta_m$	$\delta_p$
CO1° (all)	-3.1	234.1	7.4	14.8
CO1° (nor)	-3.6	228.5	17.1	33.9
CO1° (rev)	3.3	55.8	7.3	14.3
OVP <sup>1</sup>	-57.2	359.3	11.5	22.7
OVP <sup>2</sup>	59.9	76.2	17.2	32.6
IML	79.2	320.9	3.0	3.4

Lat. and Long. are latitude and longitude.  $\delta_m$  and  $\delta_p$  refer to the radius of the ellipse of 95% confidence along and perpendicular to the magnetic meridian from the site to the vertical pole.

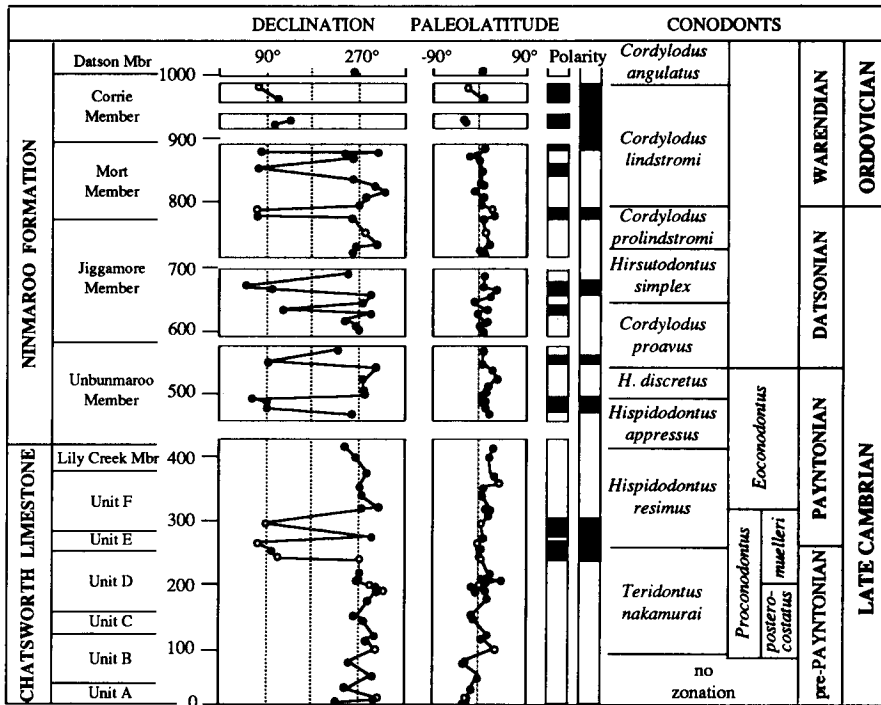


Fig. 6. Stratigraphic plot of  $CO_1^\circ$  component directions. Open circles represent endpoints of two-component demagnetization trajectories. Normal polarity zones are represented by blackened intervals. Polarity zonation on the right is the interpreted geomagnetic field behavior after the exclusion of suspect single sample polarity zones. Biostratigraphy and chronostratigraphy from Shergold & Nicoll (this volume); lithostratigraphy from Druce et al. 1982.

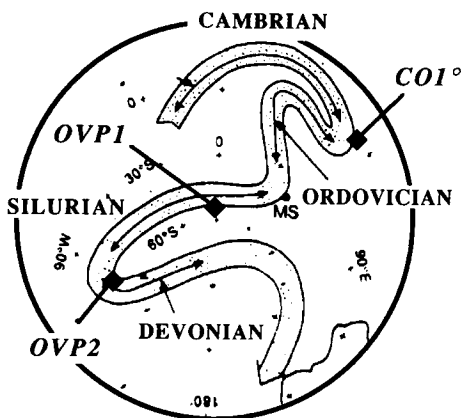


Fig. 7. Comparison of pole positions from this study with the Australian apparent polar wander track of Morel & Irving (1978).

that a hiatus might be responsible for the restricted stratigraphic range of the polarity event in BMA 86.

An argument against this interpretation is the pattern of strontium concentrations and carbon isotopes through this interval. Sample BMA 84 shows a strong enrichment in strontium, and there is a significant disruption in the stratigraphic profile of  $\delta^{13}C$  values between BMA 84 and BMA 85 (Ripperdan et al., in review). In contrast, the profile of  $\delta^{13}C$  values is not obviously interrupted between BMA 85 and BMA 86. This suggests that any depositional break would most likely have occurred between BMA 84 and BMA 85, and that the reversal preserved in BMA 86 is not the result of a hiatus.

Despite its  $CO_1^\circ$ -group direction, sample BMA 97 (625 meters) probably preserves a component of remagnetization during diagenesis.

sis. A number of the OVP samples show sharp deviations in their  $\delta^{13}\text{C}$  signature compared to their immediate neighbors possessing  $\text{CO1}^\circ$  components, as does BMA 97. Validation of this polarity event awaits further sampling, and it was not included in the interpreted polarity stratigraphy (right-hand magnetic polarity column in Fig. 6).

Samples BMA 107 (700 meters) and BMAR 430 (850 meters) both have directions that lie unambiguously within the  $\text{CO1}^\circ$  distribution. The unblocking temperature of BMAR 430 was similar to other  $\text{CO1}^\circ$  directions. However, the unblocking temperature of BMA 107 was  $500^\circ$ , more compatible with OVP-group samples. Geochemical evidence for diagenesis is absent from both samples, as opposed to many OVP samples. It is tempting to consider both as true representatives of short polarity zones but the evidence is currently not definitive, and they have been excluded from the summary magnetic polarity column.

## 5.2 Correlation

A comparison of the magnetic polarity pattern at Black Mountain with that from Dayangcha, China, shows a remarkable similarity between the two sections (Fig. 8). Both begin significant periods of normal polarity within the *Cordylodus lindstromi* Assemblage-Zone (as defined by the observations of Repetski et al., noted in Section 2), have short periods of normal polarity below the FAD of *Cordylodus proavus*, and have a normal polarity zone within the *Proconodontus muelleri* Assemblage-Zone. Important differences are found, however, including the presence at Black Mountain of the normal polarity G2+ magnetozone coincident with the *Hirsutodontus simplex* Assemblage-Zone, and the reversed polarity F2- magnetozone within strata containing the *Hispidodontus discretus* Assemblage-Zone. The apparent absence of the B group magnetozones in the Black Mountain section is most likely a function of limited biostratigraphic information from the lower 200 meters of the Chatsworth Limestone.

Polarity correlation immediately above the base of the *Cordylodus proavus* Assemblage-Zone is complicated by the presence of single sample magnetozones. One plausible correlation is between sample BMA 86 and a single

sample normal polarity zone one sample above the base of the *C. proavus* Assemblage-Zone at Dayangcha (F3+), with sample BMA 85 correlating to an underlying single sample reversed polarity zone. The coincidence of their stratigraphic positions is compelling; the samples are the lowest within the *Cordylodus proavus* Assemblage-Zone in both sections.

At Dayangcha, strata immediately beneath the base of *Cordylodus proavus* have normal polarity. However, reversed polarity characterizes the *Hispidodontus discretus* Assemblage-Zone, the equivalent level at Black Mountain. *Hispidodontus discretus* has only been recognized at Black Mountain, and stratigraphic hiatus has been suggested as one

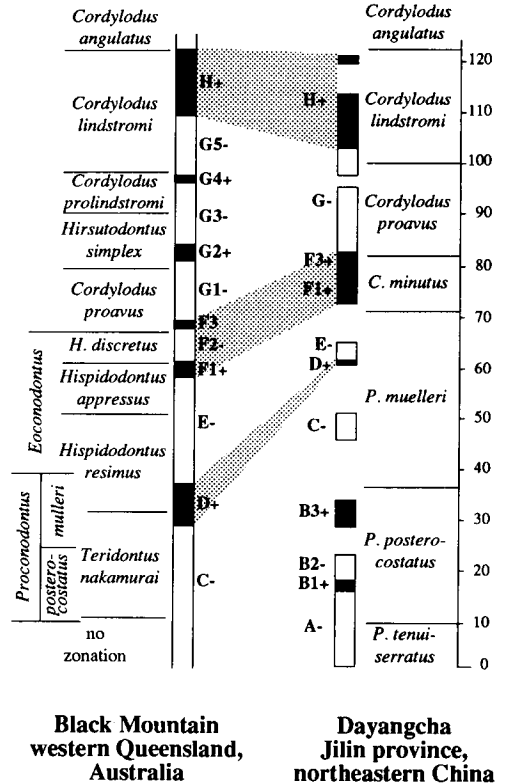


Fig. 8. Magnetostratigraphic correlation of Black Mountain to the composite section at Dayangcha. Biostratigraphy of the Dayangcha section from Chen et al. (1988) except for FAD of *Cordylodus lindstromi*, which is from Repetski, Ethington & Taylor (cited in text).

possible reason for its absence from other sections (Nicoll & Shergold 1991). Carbon isotope studies revealed no evidence of unconformity below or within the *H. discretus* Assemblage-Zone (Ripperdan et al., in review). Geochemical evidence suggests a stratigraphic break between samples BMA 84 and 85, but a hiatus at this level could not be responsible for the presence of reversed polarity below the base of *C. proavus* unless *Cambroostodus minutus*-equivalent strata were entirely absent from the Black Mountain section, and this is highly unlikely. Since the underlying *H. appressus* Assemblage-Zone at Black Mountain has normal polarity, a likely correlation between the two sections is to consider *H. discretus*-equivalent strata to be absent from Dayangcha, and correlate normal polarity within the *Cambroostodus minutus* zone to the F1+ zone at Black Mountain. If the F2-magnetozone is present at Dayangcha, it must have an extremely limited stratigraphic range; sampling intervals at Dayangcha were typically less than 0.5 meters.

The absence of the G2+ magnetozone from the section at Dayangcha presents a problem compounded by the fluctuating levels the FAD of *Cordylodus lindstromi* has assumed in recent years. *Cordylodus lindstromi* has been repor-

ted from immediately above a short interval of unsampleable strata at Dayangcha (Bed 10 of Chen et al. 1988), raising the possibility that Bed 10 may be the equivalent level of the G2+ event at Black Mountain. Because of this, it is impossible to state definitively that *H. simplex*-equivalent strata are absent at Dayangcha. However, if later work places the FAD of *C. lindstromi* below Bed 10, then the paleomagnetic evidence would strongly support the conclusion that a hiatus is responsible for the absence of the G2+ magnetozone.

There are, of course, a number of possible combinations for correlating the normal and reversed polarity zones above the base of the *Cordylodus proavus* Assemblage-Zone. However, any combination requires that significant periods of time represented by strata at Black Mountain are either in highly condensed units or are not represented within the sequence at Dayangcha. The magnetostratigraphic correlations presented are the most likely, based on the available paleontological data.

### 5.3 OVP directions

The close correspondence of OVP-group pole positions with Early Silurian and Early Devonian portions of the Australian APW (see Fig. 7) raises the possibility that periods of uplift and exposure, or alternatively, passage of diagenetic fluids, can be dated. Radke (1982, p. 251) noted that "much of the Ninmaroo Formation was exposed in the tops of domes from the mid-Paleozoic to the Jurassic." These domes were probable sites of repeated brine and hydrocarbon migration punctuated by recurring movement on existing faults (Radke 1982). Establishing a relationship between the acquisitions of secondary magnetizations and diagenetic fabrics would therefore provide a means for dating phases of structural activity in the Burke River Structural Belt.

Fig. 9 shows the distribution of OVP directions in the lower two-thirds of the Black Mountain section. OVP<sup>1</sup> directions are generally found in coarser lithologies with high original porosity, and are particularly common around the contact between the Chatsworth Limestone and the Ninmaroo Formation. OVP<sup>2</sup> directions occur with no discernible lithologic preference.

One plausible hypothesis is that OVP<sup>1</sup> direc-

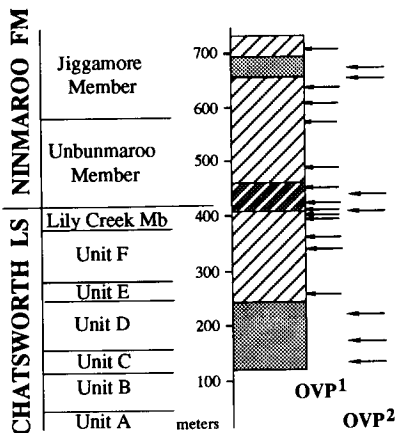


Fig. 9. Distribution of OVP directions in Black Mountain section. Crosshatched intervals contain OVP<sup>1</sup> directions; shaded intervals contain OVP<sup>2</sup> directions. Arrows indicate stratigraphic location of samples.

tions developed during fluid migration in the Early Silurian, accompanied by an occlusion of original porosity. OVP<sup>2</sup> directions could have developed during a subsequent period of fluid migration in strata less-affected by the original event. The tendency for OVP<sup>2</sup> directions to lie on the periphery of clusters of OVP<sup>1</sup> directions tends to support this hypothesis. Early phases of the Alice Springs Orogeny could easily have provided the necessary fluids and structural disruption. A definitive testing of the model, however, awaits further study.

## 6 CONCLUSIONS

A component interpreted to represent the depositional geomagnetic field is preserved within the Black Mountain sequence in polarity zones that are correlatable to the GSSP-candidate section at Dayangcha, China. The absence of *Hirsutodontus simplex* and *Hispidodontus discretus* Assemblage-Zone-equivalent polarity zones from strata at Dayangcha suggest hiatuses or highly condensed intervals at these biostratigraphic levels.

Secondary components preserved within the section are dated as Early Silurian and Early Devonian through comparison with the Australian APW track, and may eventually provide useful temporal constraints on the timing of diagenetic events within the Burke River Structural Belt.

## ACKNOWLEDGEMENTS

The authors gratefully acknowledge J.H. Shergold, R.S. Nicoll, and J. Laurie for their assistance in obtaining samples. P. Pruner and C.T. Klöotwijk are thanked for their help in preparing samples in Canberra. The advice of members of the Cambrian-Ordovician Boundary Working Group has been appreciated, and their efforts acknowledged. We wish also to thank the Bureau of Mineral Resources, Australia, for their logistical and material support. Samples from the upper part of the Ninmaroo Formation were collected by a BMR field party consisting of J.H. Shergold, R.S. Nicoll, J. Laurie, A.T. Nielsen, B.M. Radke and R.W. Brown. This work was funded in part by the National Science Foundation (grant EAR-8721391), and by the Atlantic Richfield Corp-

oration. California Institute of Technology contribution #5059.

## REFERENCES

- Chen Jun-Yuan, Qian Yi-Yuan, Zhang Jun-Ming, Lin Yao-Kun, Yin Lei-Ming, Wang Zhi-Hao, Wang Zong-Zhi, Yang Jie-Dong & Wang Yhing-Xi 1988. The recommended Cambrian-Ordovician Boundary stratotype of the Xiaoyangqiao section (Dayangcha, Jilin Province), China. *Geolog. Mag.* 125: 415-444.
- Druce, E.C. 1978. *Clavohamulus primitus* - a key North American conodont found in the Georgina Basin. *Bur. Miner. Resour. J. Austr. geol. & geophys.* 3: 351-355.
- Druce, E.C., J.H. Shergold & B.M. Radke 1982. A reassessment of the Cambrian-Ordovician boundary section at Black Mountain, western Queensland, Australia. In M.G. Bassett & W.T. Dean (eds.). *The Cambrian-Ordovician boundary: sections, fossil distributions, and correlations*, pp. 193-209. *Nat. Mus. Wales Geol. Series 3*, Cardiff.
- Epstein, A.G., J.B. Epstein & L.D. Harris 1977. Conodont color alteration - an index of organic metamorphism. *Prof. paper U.S. geol. surv.* 995: 1-27.
- Harland, W.B., A.V. Cox, P.G. Llewellyn, C.A.G. Pickton, A.G. Smith & R. Walters 1982. *A geologic time scale*. Cambridge University Press: Cambridge. 131 pp.
- Harrison, C.G.A. & B.L.K. Somayajulu 1966. Behaviour of the earth's magnetic field during a reversal. *Nature* 212: 1193-1195.
- Henningsmoen, G. 1973. The Cambrian-Ordovician Boundary. *Lethaia* 6: 423-439.
- Jones, P.J., J.H. Shergold & E.C. Druce 1971. Late Cambrian and early Ordovician stages in western Queensland. *J. geol. Soc. Austr.* 18: 1-32.
- Kobayashi, T. 1969. The Cambro-Ordovician formations and faunas of South Korea, part 10. Stratigraphy of the Chosen Group in Korea and south Manchuria and its relation to the Cambro-Ordovician formations of other areas. Section D, The Ordovician of eastern Asia and other parts of the continent. *J. Fac. Sci., Univ. Tokyo* [2], 17: 163-316.
- Li, Z.X., C.McA. Powell & G.A. Thrupp 1990. Australian Paleozoic palaeo-

- magnetism and tectonics-II. A revised apparent polar wander path and palaeogeography. *J. Struct. Geol.* 12: 567-575.
- McFadden, P.L. & M.W. McElhinny 1990. Classification of the reversal test in palaeomagnetism. *Geophys. J. Int.* 103: 725-729.
- Miller, J.F. 1984. Cambrian and earliest Ordovician conodont evolution, biofacies, and provincialism. *Geol. Soc. Amer. Special Paper* 196: 43-68.
- Morel, P. & E. Irving 1978. Tentative palaeocontinental maps for the Early Phanerozoic and Proterozoic. *J. Geol.* 86: 535-561.
- Nicoll, R.S. & J.H. Shergold 1991. Revised Late Cambrian (pre-Payntonian-Datsonian) conodont biostratigraphy at Black Mountain, Georgina Basin, western Queensland, Australia. *Bur. Miner. Resour. J. Austr. geol. & geophys.* 12: 93-118.
- Opdyke, N.D., D.V. Kent & W. Lowrie 1973. Details of magnetic polarity transitions recorded in a high deposition rate deep-sea core. *Earth & Plan. Sci. Let.* 20: 315-324.
- Pojeta, J., J. Gilbert-Tomlinson & J.H. Shergold 1977. Cambrian and Ordovician rostroconch molluscs from northern Australia. *Bull. Bur. Miner. Resour. Geol. & Geophys. Austr.* 171: 1-54, pl. 1-27.
- Radke, B.M. 1980. Epeiric carbonate sedimentation of the Ninmaroo Formation (Upper Cambrian-Lower Ordovician), Georgina Basin. *Bur. Miner. Resour. J. Austr. geol. & geophys.* 5: 183-200.
- Radke, B.M. 1981. Lithostratigraphy of the Ninmaroo Formation (Upper Cambrian-Lower Ordovician), Georgina Basin. *Rep. Bur. Miner. Resour. Geol. & Geophys. Austr.* 181: 1-141.
- Radke, B.M. 1982. Late diagenetic history of the Ninmaroo Formation (Cambro-Ordovician), Georgina basin, Queensland and Northern Territory. *Bur. Miner. Resour. J. Austr. geol. & geophys.* 7: 231-254.
- Ripperdan, R.L. 1990. Magnetostratigraphic investigations of the Lower Paleozoic system boundaries, and associated paleogeographic implications. Ph.D. thesis (unpubl.), California Institute of Technology.
- Ripperdan, R.L., M. Magaritz, R.S. Nicoll & J.H. Shergold. In review. Carbon isotope results from Black Mountain, Australia: evidence for sea level fluctuations across the Cambrian-Ordovician boundary.
- Runnegar, B.N., J. Pojeta, M.E. Taylor & D. Collins 1979. New species of the Cambrian and Ordovician chitons *Matthevia* and *Chelodes* from Wisconsin and Queensland: evidence for the early history of polyplacophoran molluscs. *J. Paleont.* 53(6): 1374-1394, 3 pls.
- Shergold, J.H. 1975. Late Cambrian and Early Ordovician trilobites from the Burke River Structural Belt, western Queensland, Australia. *Bur. Miner. Resour., Austr. Geol. & Geophys.* 153, 251 pp., 58 pl.
- Shergold, J.H. 1980. Late Cambrian trilobites from the Chatsworth Limestone, western Queensland. *Bull. Bur. Miner. Resour. Geol. & Geophys. Austr.* 186, 111 pp, 35 pl.
- Shergold, J.H. 1982. Late Cambrian (Idamean) trilobites from western Queensland. *Bull. Bur. Miner. Resour. Geol. & Geophys. Austr.* 187: 1-69, pls. 15-16.